High-performance InAs/GaAs quantum dot laser with dot layers grown at 425 °C

Li Yue (岳 丽)[1*], Qian Gong (龚 谦)[1], Chunfang Cao (曹春芳)[1], Jinyi Yan (严进一)[1], Yang Wang (汪 洋)[1], Ruohai Cheng (成若海)[1], and Shiguo Li (李世国)[2]

[1]*Shanghai Institute of Microsystem and Information Technology, Chinese Academy of Sciences, Shanghai 200050, China*

[2]*Department of Electronic Communication and Technology, Shenzhen Institute of Information Technology, Shenzhen 518172, China*

[*]*Corresponding author: yueli@mail.sim.ac.cn*

Received December 29, 2012; accepted March 28, 2013; posted online May 30, 2013

We investigate InAs/GaAs quantum dot (QD) lasers grown by gas source molecular beam epitaxy with different growth temperatures for InAs dot layers. The same laser structures are grown, but the growth temperatures of InAs dot layers are set as 425 and 500 °C, respectively. Ridge waveguide laser diodes are fabricated, and the characteristics of the QD lasers are systematically studied. The laser diodes with QDs grown at 425 °C show better performance, such as threshold current density, output power, internal quantum efficiency, and characteristic temperature, than those with QDs grown at 500 °C. This finding is ascribed to the higher QD density and more uniform size distribution of QDs achieved at 425 °C.

OCIS codes: 140.5960, 140.2020, 230.5590, 300.6360.

doi: 10.3788/COL201311.061401.

Self-assembled InAs quantum dots (QDs) as active media for laser diodes have elicited much attention because of their atomic-like quantum structures, which result in unique optical and electrical properties very different from those of traditional semiconductor lasers, such as quantum wells and bulk material lasers[1−4]. To date, most studies focus on InAs/GaAs system QD lasers; good laser performances in terms of low threshold current density, high characteristic temperature, high gain profile, large modulation bandwidth, and good wavelength stability have been obtained[5−11]. For InAs/GaAs QD lasers, growth temperature and growth equipment have important functions in the density and size uniformity of QDs, which strongly influences the performance of the laser diode. Aside from other growth techniques, such as metal organic vapor-phase epitaxy, chemical-beam epitaxy, and solid source molecular-beam epitaxy, gas source molecular-beam epitaxy (GSMBE) has also been demonstrated as a successful growth technique to obtain high-performance QD lasers[8,12,13]. In particular, the GSMBE technique has the ability to grow InAs QD on GaAs substrate in a wide range of growth temperature, thus posing a great effect on the dot density and size distribution of QDs. Joyce *et al.*[14] grew InAs QD on GaAs substrate at temperatures between 350 and 500 °C. Smaller QDs formed at 350 °C with a high density of 2.6×10^{12} cm^{-2}, whereas larger QDs were obtained at 500 °C with a low density of 5×10^{10} cm^{-2}. In general, good performance of InAs/GaAs QD lasers can be achieved by growing the QD layer at high growth temperatures of about 500 °C to obtain high optical quality. Growing QDs at low temperatures should be avoided for laser applications. However, we found that doing so may result in better device performance. In this study, we grew the same QD laser structure, but the InAs QDs were grown at 425 and 500 °C, respectively. Laser diodes were fabricated, and laser performances were characterized. The QD lasers with QDs grown at a lower temperature of 425 °C exhibit better performance than those with QDs grown at 500 °C. QDs grown at lower temperature have higher dot density and uniform size distribution, which are important for the improvement of device performance.

The samples were grown on n-type (001)-oriented GaAs substrates by GSMBE. After thermally removing the native oxide layer from the substrate, a 500-nm-thick Si-doped GaAs buffer layer was grown, followed by a 1 500-nm-thick Si-doped $Al_{0.3}Ga_{0.7}As$ cladding layer. The active region contained five-stacked InAs QD layers separated by 40-nm-thick GaAs layers. The active region was sandwiched by 20 periods of $Al_{0.3}Ga_{0.7}As$/GaAs (2 nm/2 nm) superlattices as waveguide. Finally, the structure was finished by growing a 1 500-nm-thick Be-doped $Al_{0.3}Ga_{0.7}As$ cladding layer and a 200-nm-thick Be-doped GaAs contact layer. To study the effect of QD layer growth temperature, two wafers were grown with the same structure mentioned above but with QD layers grown at 425 and 500 °C which were marked as samples A and B, respectively. To achieve desirable gain, the InAs QD deposition thickness was optimized as 1.8 monolayers (ML) for 425 °C and 2.2 ML for 500 °C. Ridge waveguide laser diodes with strip width of 10 μm and different cavity lengths were fabricated. All lasers were as-cleaved without facet coating. The chip was bonded on a copper heat-sink whose temperature can be adjusted from 20 to 60 °C. For photoluminescence (PL) measurements, the sample was excited by the 514-nm line of an Ar^+ laser. Lasing spectra were measured by a Fourier transform infrared spectrometer equipped with an InSb detector with a resolution of 0.125 cm^{-1}. The output power was measured by a Melles Griot optical power meter, including an integrating Ge detector. All measurements were carried out under continuous wave (CW) mode.

Figure 1 shows the PL spectra measured at 77 K for

 © 2013 Chinese Optics Letters

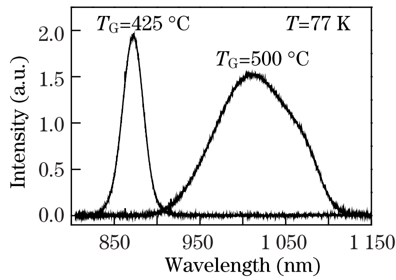

Fig. 1. Photoluminescence spectra of InAs quantum dots grown on the surface of GaAs buffer with substrate temperatures of 425 and 500 °C obtained at 77 K.

the QDs embedded in GaAs. The PL spectrum of the 1.8 ML InAs QD layer grown at substrate temperature of 425 °C is centered at 922 nm. By contrast, the PL spectrum of the 2.2 ML InAs QD layer grown at 500 °C is centered at 1 060 nm which is 138 nm longer. The central peak of the PL spectrum roughly indicates the QD sizes. Given the strong scale confinement effect in small QDs, the energy differences between the electron states and the hole states are larger than those in large QDs. Thus, smaller QDs emit photons with shorter wavelengths. Therefore, the QD size of sample A is smaller than that of sample B. The full-width at half-maximum (FWHM) of the PL spectrum at 77 K is a reflection of the QD size distribution. For more homogenous QDs, the linewidth of the PL spectrum is narrower. The FWHM of the PL spectrum for QDs grown at 425 °C is 42 meV, whereas that for QDs grown at 500 °C is 122 meV. Therefore, the QD size distribution of the sample grown at 425 °C is more homogenous than that of the sample grown at 500 °C. Therefore, growth temperature has a great impact on the size and uniformity of QDs. Growth at relatively lower substrate temperature results in smaller and more uniform QDs, similar to those from InAs/InP QDs lasers[15].

The lasing spectra at room temperature with injection current of $1.1I_{\rm th}$ are shown in Fig. 2. The laser diodes have a cavity length of 2 mm and a stripe width of 10 μm made of samples A and B, respectively, and marked as laser A and laser B. The lasing spectrum of laser A is centered at 1 025 nm, whereas that for laser B is centered at 1 084 nm, which is 59 nm longer. The result agrees well with the conclusion that QDs grown at lower temperatures have smaller sizes.

Figure 3 shows the plots of the output power from one facet versus the injection current for QD lasers A and B at 20 °C. The threshold current of laser A is 170 mA, corresponding to a threshold current density of 848 A/cm^2. Laser B has a threshold current of 197 mA, corresponding to a threshold current density of 985 A/cm^2. The QDs in sample A have smaller sizes, better size uniformity, and higher density. Thus, more QDs participate in lasing, leading to larger optical gain and lower threshold current density. The external differential efficiency $\eta_{\rm d}$ can be derived from the plots in Fig. 3 by[8]

$$\eta_{\rm d}=\frac{2q}{h\nu}\frac{{\rm d}P}{{\rm d}I}, \qquad (1)$$

where q is electronic charge, h is the Plank constant, ν is the optical frequency, and ${\rm d}P/{\rm d}I$ is the slope efficiency just above the threshold current. For laser A, the slope efficiency is 239 mW/A, the external quantum efficiency is 38.9%, and the maximum output power is 154 mW. By contrast, the performance parameters of laser B are lower, namely, slope efficiency of 170.6 mW/A, external quantum efficiency of 26.8%, and maximum output power of 93 mW.

The relationship between threshold current density and cavity length at 20 °C is shown in Fig. 4. This relationship can be expressed by[16]

$$\ln(J_{\rm th})=\ln\Big(\frac{J_{\rm tr}}{\eta_i}\Big)+\frac{\alpha_i}{g_0\Gamma}+\frac{1}{L}\frac{1}{g_0\Gamma}\ln\Big(\frac{1}{R}\Big), \qquad (2)$$

where L is the cavity length, R is the reflectivity of the cleaved facet,$\eta_{\rm i}$ is the internal efficiency, $\alpha_{\rm i}$ is the internal loss, $J_{\rm th}$ is the threshold current density, $J_{\rm tr}$ is the transparency current density, and $\ln(\frac{J_{\rm tr}}{\eta_{\rm i}})+\frac{\alpha_i}{g_0\Gamma}$ is the threshold current density for infinite length ($J_{\rm inf}$). As the cavity length of the QD laser increases, the cavity facet optical loss decreases and the laser can immediately obtain enough gain to start lasing, resulting in smaller threshold current. From the dependence of $J_{\rm th}$ on the cavity length, a threshold current density for infinite cavity length of 675 A/cm^2 is derived for sample A, corresponding to about 135 A/cm^2 per QD layer. For sample B, $J_{\rm inf}$ is 591 A/cm^2, corresponding to about 118 A/cm^2 per QD layer. From Eq. (2), the transparency current density is 394 A/cm^2 for sample A and 191 A/cm^2 for sample B. The slope of the threshold current density versus the cavity length plot of sample B is larger than that of sample A, that is, the threshold current sample

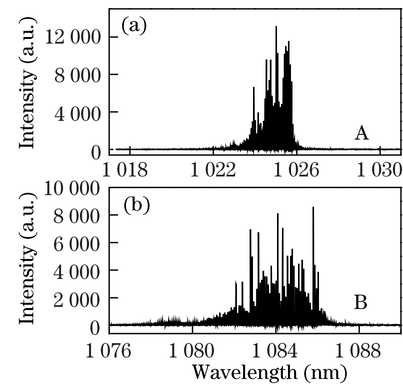

Fig. 2. Lasing spectra at 20 °C under CW mode with injection currents of $1.1I_{\rm th}$. (a) The spectrum of laser A with an injection current of 190 mA; (b) the spectrum of laser B with an injection current of 230 mA.

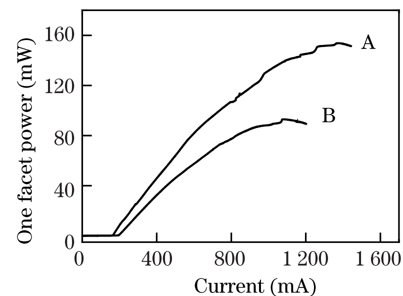

Fig. 3. Output power versus injection current under CW mode operation at 20 °C of lasers A and B.

density of sample B increases faster than that of A with decreases in the laser cavity length. For sample B, when the laser cavity length is shortened to 1.5 mm, the laser cannot operate in CW mode. For sample A, the laser with a cavity length of 0.5 mm can still work properly in CW mode. Further demonstration indicates that the optical gain of sample A is higher than that of sample B.

The internal quantum efficiency $\eta_{\rm i}$ and the internal loss $\alpha_{\rm i}$ can be derived from the dependence of external differential efficiency η_d on the cavity length as shown in Fig. 5. The relationship can be described by[8]

$$\frac{1}{\eta_{\rm d}} = \frac{1}{\eta_{\rm i}}\Big(1 + \frac{\alpha_i L}{\ln(1/R)}\Big). \tag{3}$$

For samples A and B, the internal quantum efficiencies are 72.6% and 60.4% respectively, and internal optical losses are 5.58 and 4.32 cm^{-1}, respectively. The internal quantum efficiency of sample A is higher than that of sample B because the QD density of sample A is higher and the QDs are more homogenous than those of sample B.

The temperature-dependent characteristics of the threshold current are shown in Fig. 6. The characteristic temperature of the threshold current T_0 was determined using[8]

$$J_{\rm th}(T) = J_0 \exp(T/T_0), \tag{4}$$

where $J_{\rm th}$ is the measured threshold current density, T is the heat sink temperature, and J_0 is a constant. The measurements were carried out in the temperature range from 293 to 333 K. The characteristic temperatures of laser A and laser B are 58.0 and 39.7 K, respectively, indicating that the temperature stability of laser A is better than that of laser B. The InAs QD size in laser A is smaller than that in laser B. The energy differences between the electron states and the hole states are larger because of the stronger quantum confinement of the smaller-sized QDs. The lasers with smaller QDs have better temperature stability, that is, higher characteristic temperature. As shown in the inset of Fig. 6, the slope efficiency of laser A at 60 °C is still as high as 169 mW/A, whereas the slope efficiency of laser B has declined to 124 mW/A at 50 °C. Therefore, sample A has better temperature performance than sample B.

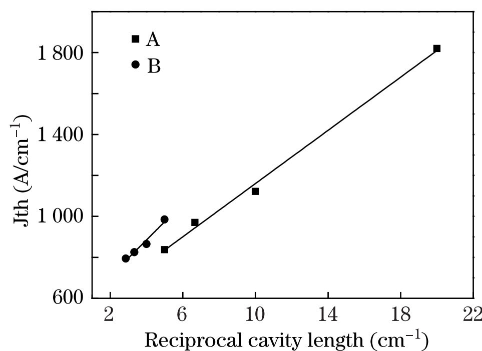

Fig. 4. Threshold current density as a function of reciprocal cavity length ($1/L$) measured at 20 °C under CW mode.

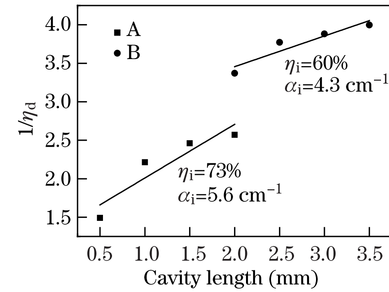

Fig. 5. Dependence of reciprocal external differential efficiency on laser cavity length at 20 °C.

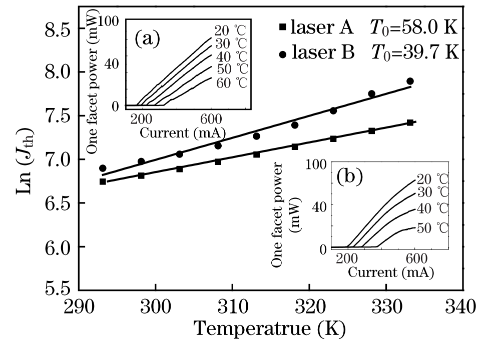

Fig. 6. Temperature dependence of the threshold current density. Insets are output power versus injection current under CW mode operation at different temperatures. (a) For laser A in the range from 20 to 60 °C; (b) for laser B in the range from 20 to 50 °C.

In conclusion, we have studied the performance of InAs/GaAs QD lasers with QDs grown at 425 and 500 °C, respectively. The output optical power, internal quantum efficiency, and characteristic temperature of the laser with QDs grown at 425 °C are all larger than those of the laser with QDs grown at 500 °C. Low growth temperature can increase QD density and improve QD uniformity, thus contributing to a narrow gain profile, increased optical gain, reduced threshold current, and improved temperature stability. These results indicate that our approach for growing InAs QD materials is effective for obtaining high-performance QD lasers.

This work was supported by the National Natural Foundation of China (Nos. 61021064, 61176065, 10990103, and 61204058) and the National Basic Research Program of China (No. 2011CB921201).

References

1. V. I. Klimov, A. A. Mikhailovsky, S. Xu, A. Malko, J. A. Hollingsworth, C. A. Leatherdale, H. J. Eisler, and M. G. Bawendi, Science **290,** 314 (2000).
2. D. Bimberg, M. Grundmann, F. Heinrichsdorff, N. N. Ledentsov, V. M. Ustinov, A. E. Zhukov, A. R. Kovsh, M. V. Maximov, Y. M. Shernyakov, B. V. Volovik, A. F. Tsatsul'nikov, P. S. Kop'ev, and Z. I. Alferov, Thin Solid Films **367,** 235 (2000).
3. S. Li, Q. Gong, X. Wang, L. Yue, O. Liu, and H. Wang, Chin. Opt. Lett. **10,** 041406 (2012).
4. M. Dezhkam and A. Zakery, Chin. Opt. Lett. **10,** 121901 (2012).

5. N. Kirstaedter, O. Schmidt, N. Ledentsov, D. Bimberg, V. M. Ustinov, A. Y. Egorov, A. E. Zhukov, M. V. Maximov, P. S. Kop'ev, and Z. I. Alferov, Appl. Phys. Lett. **69,** 1226 (1996).
6. D. L. Huffaker, G. Park, Z. Zou, O. B. Shchekin, and D. G. Deppe, Appl. Phys. Lett. **73,** 2564 (1998).
7. P. Bhattacharya, Z. Mi, J. Yang, D. Basu, and D. Saha, J. Cryst. Growth **311,** 1625 (2009).
8. S. G. Li, Q. Gong, Y. F. Lao, K. He, J. Li, Y. G. Zhang, S. L. Feng, and H. L. Wang, Appl. Phys. Lett. **93,** 111109 (2008).
9. Z. Mi, P. Bhattacharya, and S. Fathpour, Appl. Phys. Lett. **86,** 153109 (2005).
10. J. Yang, P. Bhattacharya, Z. Mi, G. Qin, and Z. Ma, Chin. Opt. Lett. **6,** 727 (2008).
11. Q. Han, Z. Niu, H. Ni, S. Zhang, X. Yang, Y. Du, C. Tong, H. Zhao, Y. Xu, H. Peng, and R. Wu, Chin. Opt. Lett. **4,** 413 (2006).
12. K. Nishi, M. Yamada, T. Anan, A. Gomyo, and S. Sugou, Appl. Phys. Lett. **73,** 526 (1998).
13. P. Caroff, C. Paranthoen, C. Platz, O. Dehaese, H. Folliot, N. Bertru, C. Labbe, R. Piron, E. Homeyer, A. Le Corre, and S. Loualiche, Appl. Phys. Lett. **87,** 243107 (2005).
14. P. B. Joyce, T. J. Krzyzewski, G. R. Bell, B. A. Joyce, and T. S. Jones, Phys. Rev. B **58,** 15981 (1998).
15. S. G. Li, Q. Gong, C. F. Cao, X. Z. Wang, L. Yue, Q. B. Liu, H. L. Wang, and Y. Wang, Infrared. Phys. Technol. **55,** 205 (2012).
16. I. L. Chen, W. C. Hsu, H. C. Kuo, H. C. Yu, C. P. Sung, C. M. Lu, C. H. Chiou, J. M. Wang, Y. H. Chang, T. D. Lee, and J. S. Wang, Jpn. J. Appl. Phys. **44,** 7485 (2005).